Fernández-Vizarra, E., Tiranti, V., and Zeviani, M. (2009). Biochim. Biophys. Acta *1793*, 200–211.

Hällberg, B.M., and Larsson, N.G. (2014). Cell Metab. *20*, 226–240.

Herrmann, J.M., Woellhaf, M.W., and Bonnefoy, N. (2013). Biochim. Biophys. Acta *1833*, 286–294.

Li, G.W., Burkhardt, D., Gross, C., and Weissman, J.S. (2014). Cell *157*, 624–635.

Mick, D.U., Dennerlein, S., Wiese, H., Reinhold, R., Pacheu-Grau, D., Lorenzi, I., Sasarman, F., Weraarpachai, W., Shoubridge, E.A., Warscheid, B., and Rehling, P. (2012). Cell *151*, 1528–1541.

Richter-Dennerlein, R., Oeljeklaus, S., Lorenzi, I., Ronsör, C., Bareth, B., Schendzielorz, A.B., Wang, C., Warscheid, B., Rehling, P., and Dennerlein, S. (2016). Cell *167*, this issue, 471–483.

Soto, I.C., Fontanesi, F., Liu, J., and Barrientos, A. (2012). Biochim. Biophys. Acta *1817*, 883–897.

Weraarpachai, W., Antonicka, H., Sasarman, F., Seeger, J., Schrank, B., Kolesar, J.E., Lochmüller, H., Chevrette, M., Kaufman, B.A., Horvath, R., and Shoubridge, E.A. (2009). Nat. Genet. *41*, 833–837.

Zhang, X., Zuo, X., Yang, B., Li, Z., Xue, Y., Zhou, Y., Huang, J., Zhao, X., Zhou, J., Yan, Y., et al. (2014). Cell *158*, 607–619.

PIWI Takes a Giant Step

Yibei Xiao[1] and Ailong Ke[1,*]
[1]Department of Molecular Biology and Genetics, Cornell University, 251 Biotechnology Building, Ithaca, NY 14853, USA
*Correspondence: ailong.ke@cornell.edu
http://dx.doi.org/10.1016/j.cell.2016.09.043

piRNA guides the action of PIWI proteins to silence deleterious transposons in animal reproductive tissues. Biogenesis of piRNA-induced silencing complex (piRISC) involves a multi-step process. In this issue, Matsumoto et al. report the first crystal structure of a PIWI-clade protein displaying a guide RNA, ready for action.

Argonaute (Ago) proteins play essential roles in small-RNA-guided processes, by silencing single-stranded (ss)RNAs complementary to its pre-loaded guide RNA (Swarts et al., 2014). They can be classified into two clades, AGO and PIWI. The AGO-clade proteins are broadly distributed and mainly interact with ~21–24 nucleotide (nt) microRNAs (miRNAs) or short interfering RNAs (siRNAs). Variants of prokaryotic Agos may target DNA, using either RNA or DNA guides (Swarts et al., 2014). The PIWI-clade proteins are narrowly expressed in animal reproductive cells and associate with ~26–30 nt PIWI-interacting (pi)RNAs to form piRNA-induced silencing complexes (piRISCs). PIWI-piRISCs protect animal germline cells by silencing deleterious transposons through either post-transcriptional degradation or transcriptional silencing (Czech and Hannon, 2016).

The biogenesis of piRNA and the assembly of PIWI-piRISC are a rather complicated process, which does not involve a double-stranded (ds)RNA intermediate as in miRNA and siRNA pathways (Czech and Hannon, 2016). Instead, the long clustered piRNA transcript is endonucleolytically cleaved, and the intermediates are loaded onto PIWI and undergo further 3′ end maturation, followed by 2′-O-methylation (2′-OME) at the 3′ terminal nucleotide (Iwasaki et al., 2015; Izumi et al., 2016) (Figure 1A). Furthermore, a unique ping-pong amplification cycle serves as a secondary piRNA biogenesis pathway, in which a subset of piRNAs is selectively amplified upon encountering transposon targets (Czech and Hannon, 2016) (Figure 1B). Studies of piRNAi have been lagging behind because the pathway is restricted to animal gonads, and the specifics of piRNA biogenesis and ping-pong mechanism vary to some extent among different systems.

Structural studies on AGO-clade proteins have generated tremendous mechanistic insights. For example, key functional states for human (h)Ago2 with or without the miRNA guide, and with the target RNA, provide the structural basis for understanding miRNAi (Schirle et al., 2014). However, similar effort on PIWI-clade Argonautes was unsuccessful. In recent years, several mechanistic breakthroughs have stemmed from studies based on the silkworm *Bombyx mori* ovary-derived BmN4 cells, which express two PIWI proteins, Siwi and BmAgo3 (Kawaoka et al., 2008). In this issue of *Cell,* Matsumoto et al. (2016) unveil the crystal structure of the silkworm Siwi-piRISC complex. The success doesn't come easy, as it involves raising a monoclonal antibody to affinity purify Siwi-piRISC directly from BmN4 cells and using a protease to release the PIWI region for structure determination. The payoff, however, is well worth the effort. The authors note structural differences of Siwi with the AGO-clade relatives, reveal piRNA recognition features, and examine the slicing mechanism. These observations lay a solid foundation for more sophisticated mechanistic dissections in the future.

Not surprisingly, Siwi bears a strong structural resemblance to its AGO-clade relatives. The four signature domains (N, PAZ, MID, and PIWI) and three linkers (L0, L1, and L2) assemble into a typical bi-lobed (N-PAZ lobe and MID-PIWI lobe) architecture found in all Ago proteins (Figure 1C). However, the relative orientation of these two lobes differs significantly between Siwi and the AGO-clade

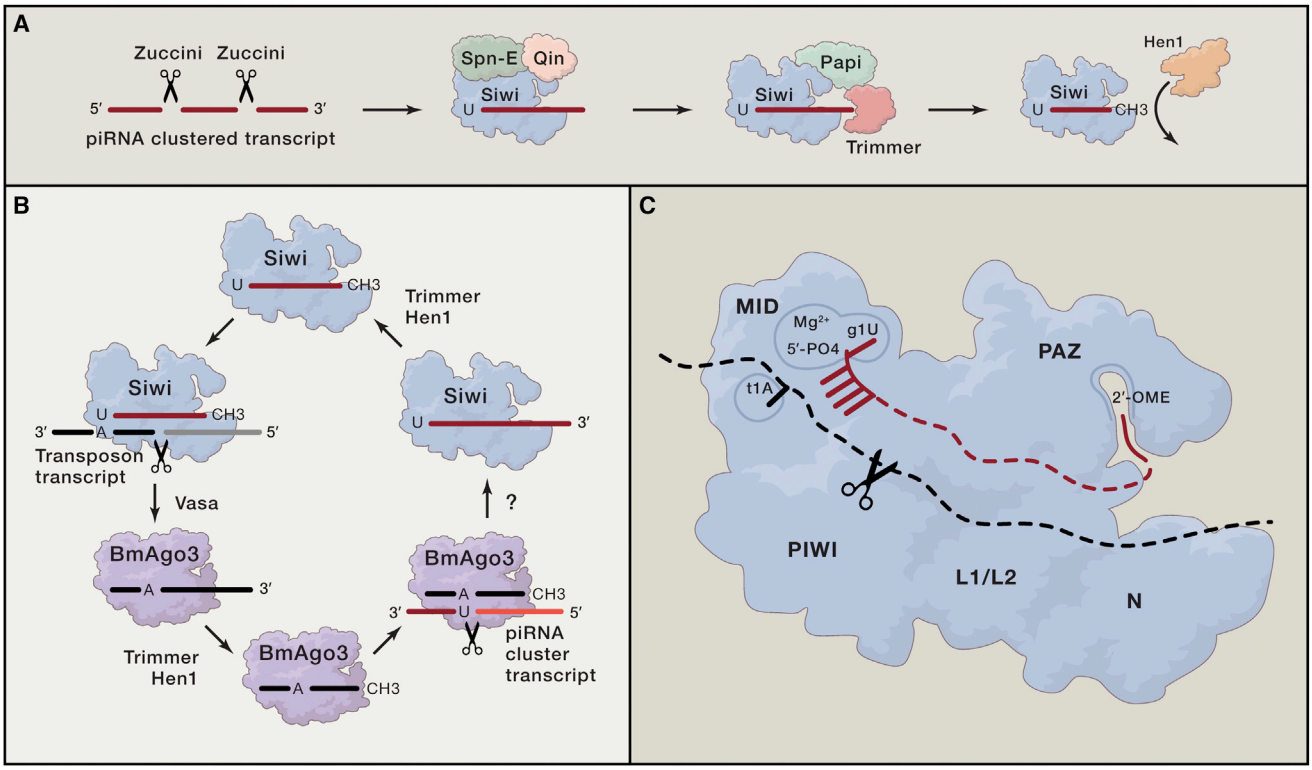

Figure 1. Schematic Diagram of piRNAi in Silkworm Ovary-Derived BmN4 Cells

(A) The primary piRNA biogenesis pathway. After nuclease Zuccini-mediated cleavage of the clustered piRNA transcript, the piRNA intermediates are loaded onto Siwi with the assistance of BmSpn-E/Qin. The subsequent binding of Papi and nuclease Trimmer defined the 3′ end of piRNA, and Hen1 further catalyzes the 2′-OH methylation (2′-OME) at the 3′ terminal nucleotide.

(B) Ping-pong amplification cycle as the secondary piRNA biogenesis pathway. When piRNA guide encounters transposon RNA target, Siwi slices at the tenth nucleotide, and nuclease BmVasa dissociates the cleavage products from Siwi. The 3′ half of the product is then loaded onto Ago3 through g10A recognition, matured therein, and guides the slicing of piRNA transcripts to specifically generate more parental piRNA guides.

(C) Siwi-piRISCs' (piRNA-induced silencing complexes) structure in a nutshell. Siwi assembles into a typical bi-lobed (N-PAZ lobe and MID-PIWI lobe) Ago architecture. It uses a tightly bound Mg^{2+} ion as part of the mechanism to read out the 5′ phosphate (5′-PO4), and an aromatic pocket to accommodate 2′-OME modification at the 3′ end. The strong preferences for a uridine at the 5′ end of guide RNA (g1U) and a complementary adenosine in the target RNA (t1A) are explained based on protein-mediated contacts. An "unplugged" catalytic tetrad is found in the PIWI domain of Siwi-piRISC. Details in target RNA recognition, cleavage, and release await further structural snapshots.

representative, hAgo2. The N-PAZ lobe in Siwi rotates significantly downward relative to its counterpart in hAgo2. Additional hinge motions between N and PAZ domains exist, due to a distinct set of contacts at the interface, which includes an AGO-clade-specific insertion. Siwi-piRISC has a robust slicing activity. The authors point out that three out of the four residues in the DEDH catalytic tetrad are well-preserved in 3D in the RNase H-fold of PIWI domain. The fourth residue, a glutamate finger in the disordered loop 2 of PIWI domain, likely joins the active site upon the guide-target RNA duplex formation. This "unplugged" active site scheme is found in Agos of some bacteria. By contrast, eukaryotic Agos contain a "plugged-in" slicer active site, in which all four residues in the catalytic triad are pre-organized.

PIWI proteins prefer a much longer RNA guide, containing a phosphate at the 5′ end and a 2′-OME modification at the 3′ end. *Drosophila* Aubergine, SIWI, and many other PIWI proteins strongly specify a uridine in the first position of their guide (g1U preference) and a complementary adenosine in the target (t1A bias). Their ping-pong cycle partner, Ago3, specifies g10A in its guide, which is equivalent to t1A before PIWI slicing; therefore, the slicing product of one naturally serves as the guide for the other, triggering an in-phase amplification cycle. In the Siwi-piRICS structure, even though the middle portion of the ~28 nt endogenous piRNA is disordered, recognitions to the sequence and chemical features at the piRNA ends are crystal clear. Siwi uses a tightly bound Mg^{2+} ion as part of the mechanism to read out the 5′ phosphate—again, a scheme not found in eukaryotic Ago, but popular among prokaryotic ones. The g1U preference is nicely explained, based on the observation that a specificity loop in Siwi MID domain flips g1U into a tightly surrounded pocket and accepts a hydrogen bond from N3 of g1U for sequence readout. A and G are too big to fit into the pocket, and C does not satisfy the hydrogen bonding pattern. As for the t1A bias, the structure supports the conclusion that t1A is specified through protein-mediated recognition, rather than base-pairing readout (Wang et al., 2014). Following g1U, SIWI

presents a stretch of four nucleotides (g2–g5) in pseudo-A form conformation. This so-called ''seed sequence region'' is much shorter than that presented by the AGO-clade proteins, hence the target searching mechanism may be somewhat different. The mechanism to accommodate 2′-OME at the 3′ end of piRNA agrees with the observations from a domain structure (Tian et al., 2011). Interactions involve a set of tyrosine residues hydrogen bonding with the 3′-OH and 2′-oxygen of the terminal nucleotide, as well as an aromatic pocket accommodating the methyl modification.

The preference for a longer guide RNA can also be rationalized to some extent. Whereas miRNA is found to travel between the MID-PIWI and N-PAZ lobes in hAgo2, no RNA densities are found in the equivalent region of Siwi-RISC. Significant slack must be present in the Siwi-bound piRNA. This is likely caused by a PIWI-clade-specific insertion into the PAZ domain, which forces piRNA outward to travel a longer path. Based on the observed MID-PIWI and N-PAZ orientation differences, the authors further speculate that the formation of the guide-target RNA duplex would cause less geometry distortion in Siwi than in hAgo2, hence the sliced product is under less pressure to release autonomously, which explains the requirement of helicases such as BmVasa in piRISC product release. Both speculations would require additional work to solidify into reliable mechanisms, by replacing structural models with real snapshots of Siwi-piRISC loaded with a homogeneous piRNA guide and programmed into the guide-target RNA duplex stage, before and after the slicing action.

In summary, the Siwi-piRICS structure ascends the mechanistic discussion of piRNAi to a higher level. Many cellular factors influence the biogenesis and functional outcome of piRISC through direct or indirect interactions with PIWI proteins. For example, in the silkworm system, nuclease Trimmer and adaptor protein Papi interact with Siwi proteins containing an sDMA modification. RNA cleavage takes place inside this ternary complex to define the 3′ end of piRNA (Izumi et al., 2016). piRNA must have traveled a different path from observed in the Siwi-piRISC structure, and the measuring mechanism inside this complex may well be the major determinant for piRNA length preference. Similarly, BmSpn-E/BmQin dimer was found to assist primary piRNA processing by interacting with Siwi, whereas a germline-specific DEAD box RNA helicase BmVasa forms complex with Siwi to facilitate the release of the sliced target RNAs from Siwi-piRISC, ensuring efficient ping-pong cycling (Nishida et al., 2015). piRISC exists in these two mutually exclusive complexes during different stages of its function cycle. Future structure and function dissections of these higher-order molecular assemblies will no doubt generate valuable insights into the piRNAi pathway.

REFERENCES

Czech, B., and Hannon, G.J. (2016). Trends Biochem. Sci. *41*, 324–337.

Iwasaki, Y.W., Siomi, M.C., and Siomi, H. (2015). Annu. Rev. Biochem. *84*, 405–433.

Izumi, N., Shoji, K., Sakaguchi, Y., Honda, S., Kirino, Y., Suzuki, T., Katsuma, S., and Tomari, Y. (2016). Cell *164*, 962–973.

Kawaoka, S., Hayashi, N., Katsuma, S., Kishino, H., Kohara, Y., Mita, K., and Shimada, T. (2008). Insect Biochem. Mol. Biol. *38*, 1058–1065.

Matsumoto, N., Nishimasu, H., Sakakibara, K., Nishida, K.M., Hirano, T., Ishitani, R., Siomi, H., Siomi, M.C., and Nureki, O. (2016). Cell *167*, this issue, 484–497.

Nishida, K.M., Iwasaki, Y.W., Murota, Y., Nagao, A., Mannen, T., Kato, Y., Siomi, H., and Siomi, M.C. (2015). Cell Rep. *10*, 193–203.

Schirle, N.T., Sheu-Gruttadauria, J., and MacRae, I.J. (2014). Science *346*, 608–613.

Swarts, D.C., Makarova, K., Wang, Y., Nakanishi, K., Ketting, R.F., Koonin, E.V., Patel, D.J., and van der Oost, J. (2014). Nat. Struct. Mol. Biol. *21*, 743–753.

Tian, Y., Simanshu, D.K., Ma, J.B., and Patel, D.J. (2011). Proc. Natl. Acad. Sci. USA *108*, 903–910.

Wang, W., Yoshikawa, M., Han, B.W., Izumi, N., Tomari, Y., Weng, Z., and Zamore, P.D. (2014). Mol. Cell *56*, 708–716.